

Studies of upper layer circulations of the South China Sea from Satellite altimeter observation

CHEN Chuntao, ZHU Jianhua, WANG He, HUANG Xiaoqi

National Ocean Technology Center, Tianjin, China P.R.

E-mail: kuroshiocct@163.com

Abstract. Seventeen years Sea Surface Current (SSC) data from multi-satellite altimeters were used to investigate the upper layer circulation structure over the South China Sea (SCS). And combined with QuikScat Sea Surface Wind (SSW) data, the relationship between upper layer circulation over SCS and SSW were analyzed. The results show that the largest current velocity and the greatest change of the circulation over the SCS are in the area east of the Indochina Peninsula; There are two main modes of the SCS upper layer circulation, the winter mode from October to next February and the summer mode from June to August. SCS circulations in other months are in the transitional period of the two main modes; Through the correlation analysis of the SSW and SSC, a significant positive correlation, about 0.5, between current and wind was found at the boundary area of the SCS. However, there was a significant negative correlation, about -0.5, near the middle of the SCS. The results also show that the variation of the upper layer circulation structure over the SCS is significant seasonal, and it was mostly dominated by the monsoon.

Keyword: South China Sea; Sea Surface Current; Sea Surface Wind; Upper Layer Circulation; Correlation Analysis; Monsoon

1. Introduction

The South China Sea (SCS) is the largest marginal sea in Southeast Asia as shown in Figure 1. It is a semi-closed basin surrounded by South China, the Philippines, Borneo Island, and the Indochina Peninsula. Deeper than 4000 m in the central region is surrounded by some shallow water areas and connects to the North Pacific Ocean through the Luzon Strait between the Taiwan Island and the Luzon Island. Semi-closed geographical characteristics make the local force to become the main driving factor in the SCS upper layer circulation^[1, 2].

The wind field in the SCS is mainly dominated by the East Asian monsoon, which is southwest monsoon in summer from the middle of May to beginning of September, and northeast monsoon in the other months. Affected by the monsoon, the SCS circulation structure showed the seasonal differences. Using the limited in-situ data, Wyrtki depicted the classic SCS circulation system^[3]; Yu used the historical temperature and salinity data further discussed the horizontal upper circulation in the SCS^[4]. Huang used the 6000 in-situ site dynamic topography data to calculate the seasonal circulation of SCS in standard layer over 1200 m^[5]. Fang et al. showed the winter and summer circulation pattern in the south of SCS^[6]. But, due to the unique geographical features in the SCS, as well as multiple spatial and temporal scale atmospheric systems effect, the SCS circulation has complex multi-temporal and spatial scales characteristics. Using the data provided by traditional observation in SCS, the spatial and



temporal changes of SCS circulation cannot be show completely; most of previous in-situ observation only covered a certain region of SCS. From the 1990s', operational spaceborne microwave altimeter can provide a long time series and large coverage data set for the study of ocean circulation, so it has therefore become an effective tool to study the SCS circulation.

Using altimeter data, previous studies described the average monthly circulation structure in the SCS and analyzed mesoscale circulation such as the Luzon cold eddy, and the western SCS summer offshore current, and believed that the monsoon was the major factor in the SCS circulation changes^[6-12]. However, most of the above studies only described mean circulation and were not concluded the duration of SCS circulation pattern and the characteristic, and not analyzed the correlationship between the wind and the SCS circulation in detail.

In this paper, the long time series altimeter data (1993 - 2009) were used to analyze the SCS circulation modes and combined the SSW data, the correlationship between the SSW and the SCS circulation was analyzed in detail.

2. Data description and data pre-processing

2.1. Altimeter data

A merged and gridded product of SSC produced by Ssalto/Duacs and distributed by Aviso based on TOPEX/Poseidon, Jason-1, ENVISAT-1, ERS-2 and JASON-2 was used here^[12]. This product has been corrected for all geophysical errors. Because the maps contain data from multiple altimeters, they are able to resolve variability on scale as small as 150 – 200 km with an accuracy of a few centimeters over most of the globe^[12]. Based on these gridded data from Jan. 1993 to Dec. 2009, the SCS upper layer circulation was studied. The gridded current dataset used in this study has a 7-day temporal resolution and a $1/3^\circ \times 1/3^\circ$ spatial resolution.

2.2. Wind data

The wind data is the product of QuikScat, distributed by IFRMER. The gridded wind dataset used in this study has a monthly temporal resolution and a $1/2^\circ \times 1/2^\circ$ spatial resolution and covers the period from January 2000 to December 2009.

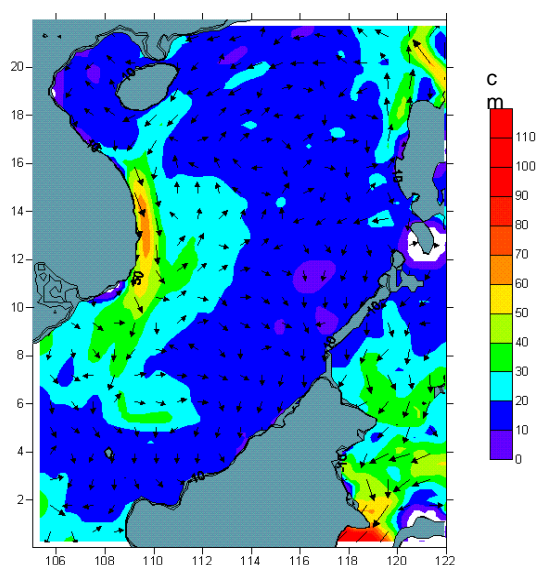
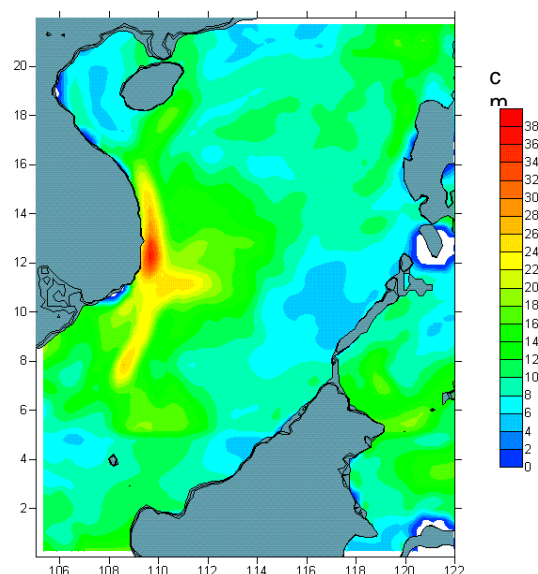
2.3. Data pre-processing

The altimeter current data have a $1/3^\circ \times 1/3^\circ$ spatial resolution, but the wind data spatial resolution is $1/2^\circ \times 1/2^\circ$. So the Kriging interpose method was used to get the same spatial resolution, $1/2^\circ \times 1/2^\circ$.

3. SCS geostrophic current

3.1. SCS climatology geostrophic current

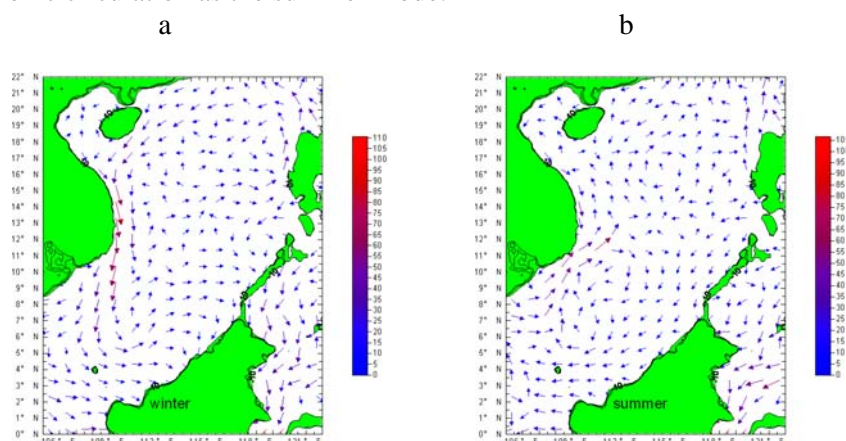
The climatology geostrophic current of SCS (Figure 1) shows that SCS upper layer circulation presents the cyclone circulation in the northern of SCS, and anticyclone circulation in the southern of SCS. There are some small-scale cyclone eddies in the northern SCS. The maximum flow rate of western boundary is near the east coastal of the Indochina Peninsula and the eastern boundary maximum flow rate appeared near the west area of the Luzon Strait. Using the standard deviation formula, the variation of monthly SCS current was analyzed. As Fig.2 shows the Standard Deviation (STD) of monthly current of SCS and the variation occurred mainly in the western boundary of the SCS and the west area of the Luzon Strait.

**Figure1.** Climatology geostrophic current of SCS**Figure2.** STD of the yearly geostrophic current of SCS

3.2. Seasonal geostrophic current of SCS

Many studies have shown that the SCS circulation have two mainly modes (summer and winter), and the change time is very short [6-11]. Unfortunately, the period of two circulation modes are not clearly divided. In this paper we used the altimeter current data from January 1993 to December 2009 to analyze the monthly change and summarize the seasonal change of the geostrophic current in the SCS and summarize the two modes' period. Then analyzed the relationship between the current and the wind in SCS.

Through the 12 monthly geostrophic current analyzed, we can get the following conclusions: Overall: SCS upper layer circulation presents the cyclonic circulation from October to next February, transition period from March to May, the anticyclonic circulation from June to August, and September is transition period. So we concluded the cyclonic circulation as the winter mode of SCS circulation, and the anticyclonic circulation as the summer mode.

**Figure3.** Two main modes of SCS Circulation. a is the winter mode of SCS Circulation and b is the summer mode.

From October to next February, the SCS circulation is in the winter mode (Figure 3a), which presents the cyclonic circulation. The strong SCS monsoon jet is the characteristics of the winter SCS circulation, which turn to northeast at the Sunda Shelf. In winter mode, northeast monsoon produces

the wind-drift current with the southern direction. Ekman transport caused by wind-drift current affects with the right side land and accumulates in the right side of the current, then produces a barotropic pressure gradient force from coastal toward to offshore which caused a geostrophic current with a same direction of wind-drift current. The same direction of geostrophic current and wind-drift current produce the strong nearshore jet. So the nearshore jet emerging from October to next February can be used as the characteristics of the winter mode of SCS circulation.

From June to August, the SCS circulation summer mode (Figure 3b) presents the anticyclonic circulation. The strong northeast current near the southwest of Indo-China Peninsula is the characteristics of the summer SCS circulation. In the northern of SCS the current presents cyclonic, and the southern SCS presents anticyclonic. In summer mode, southwest wind produces the northern direction wind-drift current. Ekman transport of wind-drift current causes the nearshore sea level reduces and forms an upwelling current, then produces a baroclinic pressure gradient force from offshore toward to coastal which caused a geostrophic current with a same direction of wind-drift current. The same direction of geostrophic current and wind-drift current form the nearshore jet. So the nearshore jet emerging from June to August can be used as the characteristics of the summer mode of SCS circulation.

From March to May, it was the transition period for SCS circulation from winter pattern to summer pattern. The southern current at SCS west boundary continually weakens, and a southwest current gradually generated near the southwest of Kalimantan Island. Cyclonic circulation appeared in the north SCS and an anticyclonic circulation appeared in the middle and south SCS respectively. September was the transition period for SCS circulation from summer pattern to winter pattern. The characteristic of that period was the appearing of the strong SCS monsoon jet and the weakening of southwest current near the Indo-China Peninsula, those currents combined together flowed toward northeast, and crossed the whole middle SCS.

4. Correlation analysis of geostrophic current and wind

SCS is located in the monsoon region, which meridional axis is consistent with the monsoon, easily to produce the wind-drift current^[8-11]. So the wind data were used to analyze the correlation coefficient between circulation and wind in the SCS. In section 3, the SCS circulation have been analyzed, there are two most important modes, winter mode and summer mode. The relationship between circulation and wind was analyzed during the two modes period. Compared the monthly wind and current data, good agreement in trends was concluded between current and wind.

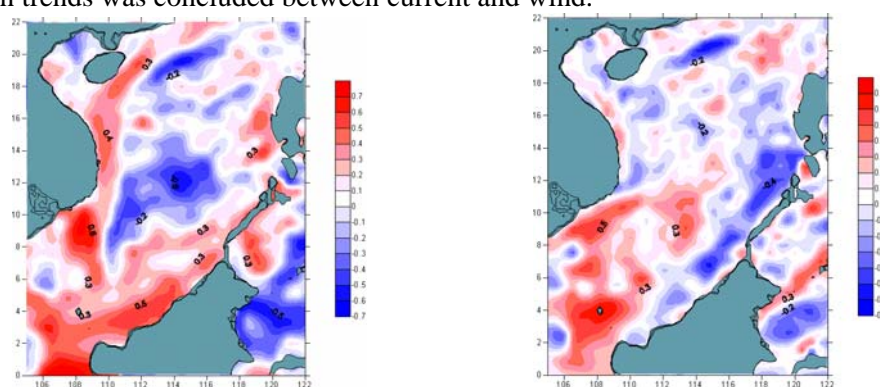


Figure 4. The correlation coefficient between circulation and wind in the SCS in two mainly modes. Left is correlation coefficient field of the winter mode of SCS circulation, and right is correlation coefficient field of the summer mode of SCS circulation.

Using the wind and current data of SCS from 2000 to 2009, the relationship of wind and current was analyzed, showed as Figure 4 and 5. Fig. 4 shows the correlation coefficient between circulation and wind in the SCS in two mainly modes. Left is correlation coefficient field of the summer mode of SCS circulation, and right is correlation coefficient field of the winter mode of SCS circulation.

In the winter mode, current and wind have a positive correlation and the coefficient is 0.5 at the boundary of SCS, have a -0.5 correlation coefficient at the center of SCS. As analyzed in section 3.2 SSW produces a wind-drift current, which has the same direction of geostrophic current in the west boundary of SCS, so there is a positive correlation and the coefficient is 0.5 at the west boundary of SCS. So the positive 0.5 correlation coefficient can be used to prove the nearshore jet emerging as the characteristics of the winter mode of SCS circulation.

In the summer mode, current and wind have a positive correlation and the coefficient is 0.5 at the boundary of SCS, have a -0.5 correlation coefficient at the center of SCS. As analyzed in section 3.2 SSW produces a wind-drift current, which has the same direction of geostrophic current in the west boundary of SCS, so there is a positive correlation and the coefficient is 0.5 at the west boundary of south SCS and nearshore jet emerging near the Indochina Peninsula can be used as the characteristics of the summer mode of SCS circulation.

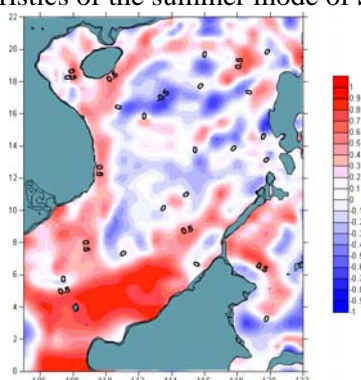


Figure 5. The correlation coefficient between yearly average circulation and wind in the SCS

There is a positive correlation of Climatology geostrophic current and wind, and the maximum correlation coefficient is 0.5 in the boundary of SCS, and Negative correlation in middle of SCS with the -0.5 correlation coefficient.

5. Summary

Seventeen years altimeter data were used to analyze the seasonal and monthly variation of SCS circulation. Combined with wind data, the characteristics of SCS was analyzed, and concluded as below: Basing on the seventeen years monthly average circulation of SCS, the SCS circulation was concluded in two main modes, the winter mode from October to next February and the summer mode from June to August. SCS Circulations in other months are the transitional of the two main modes. The SCS circulation winter mode presents the cyclonic circulation. The strong SCS monsoon jet is the characteristics of the winter SCS circulation, which turn to northeast at the Sunda Shelf. The SCS circulation summer mode presents the anticyclonic circulation. The strong northeast current near the southwest of Indo-China Peninsula is the characteristics of the summer SCS circulation. In the northern of SCS the current presents cyclonic, and the southern SCS presents anticyclonic. There is a positive correlation of Climatology geostrophic current and wind, and the maximum correlation coefficient is 0.5 in the boundary of SCS, and Negative correlation in middle of SCS with the -0.5 correlation coefficient.

6. Acknowledgement

This study was supported by the Marine Public Welfare Project of China under contract No. 201305032-3 and 201105032-5; the authors would thank the AVISO for providing Altimeter data, the IFRMER for providing wind data respectively.

7. References

- [1] Li Li 2002 Advance in observational studies of upper layer circulations of the South China Sea, *Journal of oceanography in Taiwan Strait*, **21**, **1** pp 114-125
- [2] Guo Junjian, Fang Wendong, Fang Guohong, Chen Haiying 2006 Variability of surface circulation in the South China Sea from satellite altimeter data, *Chinese Science Bulletin* **51 Supp. II 1** pp 1-8.
- [3] Wyrski K 1961 Physical oceanography of the Southeast Asian waters. *NAGA Rep 2. Scripps Institute of Oceanography*, LaJolla, CA, USA, 195
- [4] Yu Mugeng and Liu Jinfang 1993 Circulation system and trend in the South China Sea, *MARINE FORECASTS* **10**, **2** pp 13-17
- [5] Huang Qizhou, Wang Wenzhi 1992 General Situations of the current and eddy in the South China Sea, *Advance in earth sciences*, **7**, **5** pp 1-9
- [6] Fang Wendong and Fang Guohong 1998 The recent progress in the study of the southern South China Sea circulation, *ADVANCE IN EARTH SCIENCES*, **13**, **2** pp 166-172
- [7] Mao Qingwen, Shi Ping, Qi Yiquan 1999 Sea surface dynamic topography and geostrophic current over the South China Sea from Geosat altimeter observation, *ACTA OCEANOLOGICA SINICA*, **21**, **1** pp 11-16
- [8] Qi Yiquan and Shi Ping 1999 Analysis on Monthly average distribution characteristics of Sea Surface Wind and Wave in South China Using Altimeter data, *TROPIC OCEANOLOGY*, **18**, **2** pp 119-124
- [9] Li Li, Wu Risheng, Guo Xiaogang 2000 Seasonal circulation in the South China Sea a TOPEX / POSEIDON satellite altimetry study, *ACTA OCEANOLOGICA SINICA*, **22**, **6** pp 13-26
- [10] Liu Qinyu, Jia Yinglai, Yang Haijun, Liu Zhengyu 2002 Seasonal variation mechanism of sea surface height in the north of the SCS, *ACTA OCEANOLOGICA SINICA* **24**, **1** pp 9-17
- [11] Wang Jing, Qi Yiquan, Shi Ping, Mao Qingwen, Zhu Peter 2003 Characteristics of Sea Surface Height in South China Sea based on data from TOPEX/POSEIDON, *Journal of Tropical Oceanography*, **22**, **4** pp 26-33
- [12] Ducet, N., Le Traon, P.Y., Reverdin, G. 2000 Global high resolution mapping of ocean circulation from TOPEX/Poseidon and ERS-1 and -2. *J. Geophys. Res.* **105** (C8) pp 19477 - 19478.